Effect of Oil-Water Intermittent Wetting on Corrosion Inhibition of Carbon Steel in CO_2 Environment

Yi He,[‡,] Xi Wang,[*] Luciano Paolinelli,[*] David Young,[*] Maalek Mohamed-Saïd,[**] and Marc Singer[*]*

Produced water can cause internal corrosion in oil pipelines. The flow of hydrocarbons and water can result in intermittent surface wetting, impacting corrosion inhibition. However, this is still poorly understood. This research uses electrochemical techniques to study the impact of intermittent wetting and the wettability of the steel surface on corrosion inhibition. An inhibitor model compound and model oil were used at 25°C and 55°C in CO_2-saturated solutions. Corrosion inhibition varied with temperature and steel surface hydrophobicity, altering inhibition significantly after intermittent contact with hydrocarbon at 55°C. Electrochemical impedance spectroscopy and wettability results revealed distinct protective mechanisms when oil was present.

KEY WORDS: carbon dioxide, corrosion inhibitor, electrochemical impedance spectroscopy, hydrocarbon, intermittent wetting, wettability

INTRODUCTION

In the oil and gas sector, the typical method for transporting petroleum and its derivatives over extensive distances involves using large-diameter pipelines made of carbon steel. The existence of produced water within the oil carries the risk of causing significant corrosion to the internal walls of transmission systems.[1] The flow of hydrocarbons and water can exhibit diverse and intricate regimes, where intermittent surface wetting by water and oil phases can occur.[2] In the refinery, outlet upper column where filming amines are used, alternate wetting with oil is likely. A highly efficient approach to control corrosion involves the continuous injection of corrosion inhibitors (CIs) into pipelines transporting oil-water mixtures. As corrosion occurs on metal surfaces exposed to water, the molecules of CI can form adsorbed layers that retard electrochemical reactions at the interface between water and metal.[3] Consequently, this process protects carbon steel pipes from corrosion caused by CO_2 and H_2S.

The adsorption of organic molecules onto surfaces via heteroatom functionalities, such as nitrogen, oxygen, sulfur, and/or phosphorus, can significantly alter the corrosion resistance properties of metals. Among these organic compounds, heterocyclic molecules containing nitrogen atoms have proven to be exceptional CIs for numerous metals and alloys across various harsh environments.[4-6]

Some limited attention has been given to the subject of how inhibitors interact with hydrocarbon in oil-water intermittent wetting. Li, et al.,[7] studied corrosion inhibition using a glass cell with a rotating cylinder electrode in the water phase only and also adding the hydrocarbons on top of the brine phase to produce alternate exposure to oil after inhibitor addition. The corrosion rate (CR) was found to decrease sharply for a fatty amine inhibitor after the sample was exposed intermittently to the hydrocarbon phase. This effect was associated with the formation of a hydrophobic inhibitor layer at the steel surface that was strengthened by the interaction with the inert model oil molecules.[8]

Intermittent wetting of carbon steel by oil can affect the inhibitor adsorption dynamics and protective layer formation, and consequently the inhibition mechanism. However, there is no specific explanation for the phenomena that occur at the metal/film and film/solution interfaces under different conditions (i.e., different surface wettability). In addition, most studies about CI performance in intermittent wetting only focused on ambient conditions without considering higher temperatures.[7-9] Therefore, there is a need to investigate further to cover the factors mentioned above.

Electrochemical impedance spectroscopy (EIS) has proven to be a powerful technique for studying the adsorption and formation of CI layers and corrosion inhibition mechanisms.[10-11] Physical phenomena, such as the corrosion process, inhibitor film formation, and growth can be modeled and interpreted using equivalent electric circuits, which can help to identify the controlling mechanisms, to fit the experimental impedance spectra as shown elsewhere.[12] Nevertheless, there is scant reporting of EIS utilization for corrosion inhibitor evaluation in the presence of oil in the literature. A study conducted by Sonke and Bos,[13] mimicking oil and gas production environments, successfully applied EIS to monitor the formation of protective layers on carbon steel exposed to water with hydrocarbons and an imidazoline-type CI. However, this work was not conducted over a wide range of temperatures and only outlined experimental conditions and results, with limited analysis and interpretation of the generated data. He, et al.,[14] monitored the inhibitor film buildup with EIS on the intermittent oil

Submitted for publication: April 05, 2024. Revised and accepted: May 26, 2024. Preprint available online: May 29, 2024, https://doi.org/10.5006/4575.
‡ Corresponding author. E-mail: yh429518@ohio.edu.
* Institute for Corrosion and Multiphase Technology, Department of Chemical and Biomolecular Engineering, Ohio University, Athens, Ohio, 45701.
** TotalEnergies, OneTech, CSTJF, Avenue Larribau, F-64018 Pau, France.

ISSN 0010-9312 (print), 1938-159X (online)

Table 1. *Composition (wt%) of Carbon Steel C1018*

Element	Cr	Mo	S	V	Si	C	Ni	Mn	P	Fe
Wt%	0.076	0.015	0.026	0.001	0.21	0.15	0.027	0.63	0.011	Balance

or water-wetted carbon steel surface. They found that the chloride concentration played a crucial role in the film structure, and oil interacted with the adsorbed inhibitor film. However, the impact of oil on corrosion inhibition was not further investigated in their work.

Contact angle measurements have been used to characterize the wettability of steel surfaces in contact with water and hydrocarbons.[15] This method can be utilized to directly observe the behavior of the three-phase system (water, oil, and metal) and to measure the tendency of water to displace hydrocarbon from steel.[16-17] Contact angle measurements measure the angle formed between the tangent to the droplet and the solid surface at the point of contact. Li, et al.,[7] established that fatty amine and quaternary ammonium chloride inhibitor compounds altered the wettability of carbon steel from hydrophilic to hydrophobic as their concentration increased. This was in line with an improvement in corrosion inhibition when hydrocarbon was present for inhibitors that promoted more hydrophobicity. Schmitt and Stradmann[18] studied the wettability of steel surfaces at 75°C and 80°C and 5 bar CO_2, while also investigating the impact of CIs and other surface-active compounds. They found that quats, amines, and imidazolines influenced the hydrophilic/hydrophobic properties of corroding carbon steel. Foss, et al.,[19] studied the effect of the inhibitor/oil interactions in CO_2 corrosion tests, where the steel specimens were alternately exposed to oil and the aqueous phase. They observed that the inhibitors enhanced the oil wettability of the steel surface using the contact angle measurement, and the inhibition was significantly improved by the presence of oil. However, there are several limitations of the contact angle method. This method depends on the sequence of fluid introduction and is difficult to conduct at elevated pressure or with dark oil backgrounds.[20] An alternate method is the spreading method,[16] which involves measuring the electrical resistance between isolated steel pins wetted by the oil-water mixture. When a conducting phase (e.g., water) covers the distance between the pins, the conductivity between them will be high, whereas a nonconducting phase (e.g., oil) will result in low conductivity. Papavinasam, et al.,[20] studied the effect of hydrocarbons on the internal corrosion of oil and gas pipelines, results indicated that the spreading method better differentiates hydrocarbons in terms of their wettability than the contact angle method. They established that it is difficult to perform contact angle measurements at elevated pressures and under flow conditions. However, in their study, the measurements were conducted over 24 h of exposure, which is much longer than for contact angle measurements. The spreading method helps to identify water-oil wetting conditions and can be used to determine if the metal is hydrophobic or hydrophilic, but it does not provide a criterion to characterize its hydrophilic/hydrophobic character. While this approach is suitable for certain applications, it does not offer detailed insights into interfacial phenomena or the underlying mechanisms governing wetting behavior, as compared to the contact angle method. Moreover, as the current work was conducted at 1 bar CO_2 using LVT 200[†] model oil with no dark oil background, and using 50 g/L NaCl with 1,000 rpm rotational speed, this mitigates some of the challenges associated with contact angle measurements. Consequently, the contact angle method was used in this study to provide valuable insights into wettability characteristics crucial for the study.

In the oil and gas sector, produced water during the extraction of hydrocarbons from wells often contains elevated levels of dissolved salts. Apart from salts, corrosive gases like CO_2 are present in the production stream, dissolving into the produced water. This process acidifies the solution, posing a risk of internal corrosion in pipelines. While there are indeed many other ions present in oilfield-produced water, this work focuses on elevated salt concentration (5 wt% NaCl), simulating the conditions found in the exploration and production environments within the oil and gas industry, but without complicating cations and anions (e.g., Ca^{2+}, Mg^{2+}, Sr^{2+}, SO_4^{2-}, etc.); these can induce additional phenomena during experiments, such as bulk precipitation or scale formation, that can impact corrosion inhibition studies. This paper presents an experimental methodology that uses electrochemical techniques, particularly EIS and contact angle measurements. The focus is on investigating the effects of intermittent wetting, simulating multiphase flow phenomena, on corrosion inhibition. Particularly, the corrosion inhibition of carbon steel at 25°C and 55°C in a CO_2-containing environment with intermittent wetting with oil was characterized and analyzed using linear polarization resistance (LPR), potentiodynamic sweeps, and EIS. The steel surface wettability at different temperatures was investigated by measuring the contact angle of sessile oil droplets in the water phase.

EXPERIMENTAL PROCEDURES

2.1 | Materials and Chemicals

C1018 (UNS G10180[(1)]) carbon steel specimens featuring a ferritic-pearlitic microstructure were used for the entirety of the tests. Table 1 displays the composition of this carbon steel.

The hydrocarbon phase utilized in this study was LVT 200, a transparent and light paraffinic distillate composed primarily of straight-chain hydrocarbons (C9–C16), with C14 being the predominant fraction. Its dynamic viscosity and density were 2.7 cP and 823 kg/m^3, respectively. The hydrocarbon did not contain any impurities which could act as a CI.

A CI model compound, tetradecyltetrahydropyrimidinium (THP-C14), was synthesized in-house with a purity exceeding 99%, as described in a prior publication.[21] THP-C14 is found in particular commercial CI formulations for the oil and gas industry, its chemical structure includes a positive charge in the head group that delocalizes between two nitrogen atoms, with a $-C_{14}H_{29}$ tail.[21] The aqueous solution was prepared using certified ACS grade NaCl (Fisher Chemical™[†], NJ) and ASTM Type II deionized (DI) water.

2.2 | Electrochemical Measurements

Electrochemical experiments were conducted using a three-electrode glass cell setup equipped with a hot plate (Figure 1). The working electrode used was a C1018 rotating

[†] Trade name.

[(1)] UNS numbers are listed in *Metals and Alloys in the Unified Numbering System*, published by the Society of Automotive Engineers (SAE International) and cosponsored by ASTM International.

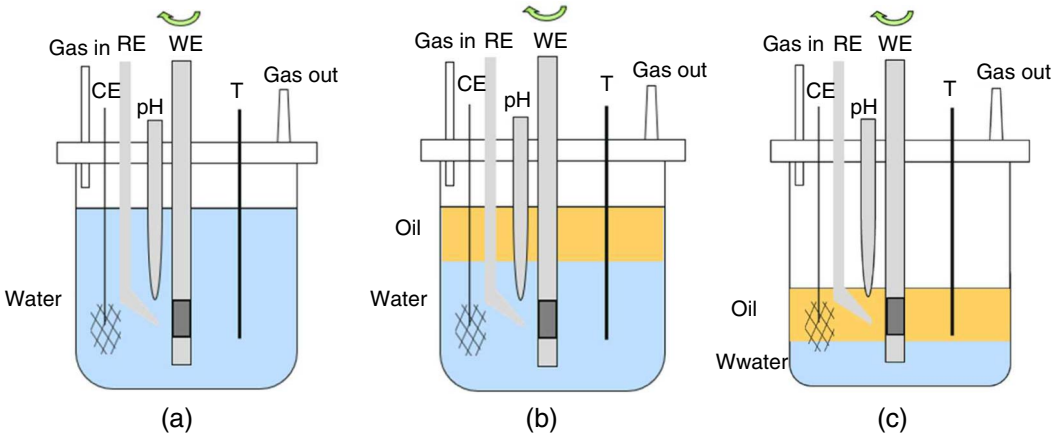

FIGURE 1. *Schematic of the three-electrode glass cell setup used for corrosion inhibition experiments. "Gas in" and "gas out" are where CO_2 continuously flows through the glass cell. "CE", "RE", and "WE" are the counter electrode, the reference electrode, and the working electrode, respectively. "T" is the thermocouple. (a) Pure water wetting experiments, (b) water-wetting stage in oil-water intermittent experiments, and (c) oil-wetting stage in oil-water intermittent wetting experiments.*

cylinder electrode (RCE) with an exposed area of 2.76 cm^2, a platinum-coated titanium mesh counter electrode, and an Ag/AgCl (KCl saturated) reference electrode. Before each experiment, the RCE was sequentially polished with #240, #400, and #600 grit SiC abrasive papers and DI water, cleaned with isopropanol in an ultrasonic bath, and then air-dried. The rotational speed of the RCE specimen was adjusted to 1,000 rpm utilizing a modulated speed rotator (Pine Research Instrumentation™†). The rotational speed of 1,000 rpm was selected based on consultation with sponsors. This speed simulates typical operational parameters encountered in industrial settings and reflects exploration production conditions relating to flow phenomena.

Electrochemical measurements were conducted using a Gamry Reference 600™† potentiostat. The CR was determined by measuring LPR with a scan potential range of −5 mV_{OCP} to +5 mV_{OCP} (open-circuit potential) at a scan rate of 0.125 mV/s. B value of 26 mV, taken from previous research with mild steel in a CO_2 environment,[22] was used to convert LPR data to CR for all of the tests reported herein. The B value for inhibited and uninhibited conditions in a system with or without oil could be different due to the change of dominance of mass transfer and charge transfer on the cathodic reaction. In the absence of an inhibitor, a B value of 26 mV has been proposed to represent CO_2 corrosion environments that are often mixed charge transfer and the reaction of mass transfer controlled.[23] Analysis of all the potentiodynamic polarization sweeps performed in this study in the presence of an inhibitor showed a range of B values varying from 17 mV to 21 mV, depending on the experimental conditions. However, for the sake of simplicity of a CR calculation, the B value of 26 mV was consistently applied to analyze all of the experimental data reported in this study. It is understood that this assumption could lead to an overestimation of the CR in the presence of an inhibitor of up to 30%—yet this would not alter the main findings of this work as inhibited steady state CR are typically very low. The measured polarization resistance (R_p) was compensated with the solution resistance (R_s), which was determined by EIS. EIS measurements were performed at OCP with an amplitude of perturbation of 10 mV_{RMS}, and a frequency range of 10 kHz to 0.1 Hz. Potentiodynamic polarization curves were collected at the end of the experiments. The cathodic and anodic sweeps were obtained separately by polarizing from OCP to approximately −0.7 V and +0.2 V, respectively, and with a scan rate of 0.125 mV/s. Table 2 shows the parametric matrix for the electrochemical tests.

Two different experimental procedures, including pure water wetting and intermittent wetting, were followed for the inhibition experiments with electrochemical measurements. The details of the procedures were provided previously.[14] During the pure water wetting experiments, the RCE sample was constantly immersed in the water phase without any presence of hydrocarbon in the glass cell (Figure 1[a]). For the intermittent wetting experiments, the electrolyte level was adjusted by extracting electrolytes to immerse the RCE sample in the water phase (Figure 1[b]) and the oil phase (Figure 1[c]) alternately. The specimen underwent a 1-h rotation at 1,000 rpm in the oil phase, which was long enough to allow the sample surface to reach a steady state; oil phase exposure times as low as 20 min in separate experiments yielded similar results. The electrochemical measurements were conducted in the water phase only, any readings directly from the oil phase would be invalid due to the impeded charge transfer within this media. The inhibitor was injected into the electrolyte for both procedures, and oil was applied on top of the electrolyte for the intermittent wetting experiments. LPR and EIS were collected periodically during both procedures. After each experiment, potentiodynamic polarization curves were collected. Each experiment was replicated at least twice.

2.3 | Contact Angle Experiments

The contact angle measurements were conducted using a goniometer[24] equipped with heating capabilities. The goniometer consisted of a stainless-steel cell featuring flat glass windows for the visual inspection of internal fluids, and a holder to place the test specimen. The cell contained ports at its bottom and top for droplet injection, insertion of pH probe, gas sparger tube and thermocouple, and drainage. A digital image capture system was used with a backlight to enhance image illumination and contrast.

As the THP-C14 model inhibitor described in this study is cationic,[21] the results presented in this work focus on the oil-in-water contact angle. For each tested condition, the test cell was filled with 500 mL of 5 wt% NaCl solution. The solution was deoxygenated with CO_2 gas for more than 1 h and pH was

Table 2. *Matrix for Electrochemical Experiments*

Description	Parameters
Electrolyte	5 wt% NaCl
Working electrode	Carbon steel UNS G10180 (C1018)
Sparge gas	CO_2
Temperature	25°C and 55°C
pH	4.5±0.1
CI model compound	1-tetradecyl-1,4,5,6-tetrahydropyrimidinium bromide (THP-C14)
Inhibitor concentration	0.5 ppm at 25°C and 25 ppm at 55°C
Oil type	LVT 200 model oil (hydrotreated light distillate C9–C16)
RCE rotational speed	1,000 rpm

adjusted to 4.5 using the procedure mentioned in the *Electrochemical Measurements* section above. A flat C1018 carbon steel sample was finished with #600-grit SiC paper, followed by sonication in isopropanol, air drying, and subsequent placement on a polytetrafluoroethylene (PTFE) sample holder within the goniometer, with its prepared surface facing the bottom of the cell. After the sample was immersed in the brine phase, the CO_2 sparger tube was lifted above the liquid line to avoid the potential presence of gas bubbles on the test surface. The oil droplets were placed onto the specimen surface using a volume-calibrated glass syringe with a long stainless-steel needle.

Baseline experiments without inhibitors were performed first, and then a series of tests with different THP-C14 inhibitor concentrations in the water phase were performed afterward. A minimum of two independent tests with three injected 10-µL oil droplets each were used to measure the contact angle for all of the covered experimental conditions. The Bond number calculated for the droplet, considering its nondeposited radius, was 0.08. This value was sufficiently low to prevent both gravity-induced shape distortion of the sessile droplet and any errors in the measured contact angles.[25] The contact angles of the sessile droplets were estimated by the truncated sphere method:[24]

$$\frac{c'}{h'} = \frac{\sin\theta}{1-\cos\theta} \quad (1)$$

where θ is the contact angle measured from inside of the droplet as shown in Figure 2, h′ is the droplet height, and 2c′ is the contact base length. These values were obtained from the captured digital images using IC MEASURE®†. Figure 2 shows examples of oil-in-water contact angles of sessile droplets for a hydrophilic surface (preferentially water-wet with a high contact angle >90°) and a hydrophobic surface (preferentially oil-wet with a low contact angle <90°).

RESULTS AND DISCUSSION

3.1 | Linear Polarization Resistance Results

3.1.1 | Pure Water Wetting

Before investigating intermittent wetting, a full characterization of the behavior of the inhibitor in aqueous solution

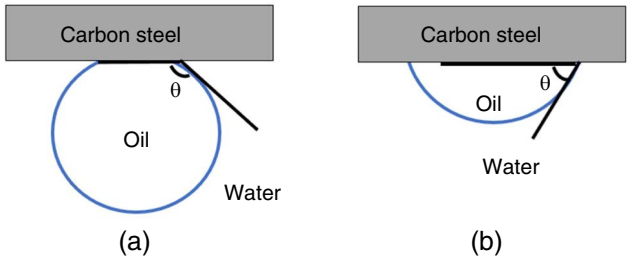

FIGURE 2. *Sketch of oil-in-water contact angles θ of sessile droplets on (a) hydrophilic and (b) hydrophobic carbon steel surfaces.*

(no oil) needed to be completed. The performance of the THP-C14 inhibitor was assessed in pure water wetting conditions using different THP-C14 concentrations at 25°C and 55°C.[26] Table 3 summarizes the obtained steady-state CR (i.e., final stable values). From the CR measurements over the various used inhibitor concentrations, metal surface saturate concentration (MSSC) values were determined, above which the CR could not be further reduced upon increasing inhibitor concentration. The MSSC of THP-C14 was found to be between 1 ppm and 4 ppm at 25°C, whereas, at 55°C, it was determined between 50 ppm and 70 ppm.[26] For comparison purposes, Table 3 also lists inhibitor efficiency (E_{CI}) values (%) based on Equation (2):

$$E_{CI} = 100\left(1 - \frac{CR_i}{CR_o}\right) \quad (2)$$

where CR_i and CR_o are the final CR with and without inhibitor addition.

It is worth noting that when the inhibitor concentration was higher than MSSC, the CR was below 0.1 mm/y. This CR value was already too low to further observe and distinguish any beneficial effect of hydrocarbon wetting on corrosion inhibition. Therefore, to facilitate the study of any inhibition enhancement by intermittent oil wetting at 25°C and 55°C, all of the selected inhibitor concentrations were below the MSSC, where the CR were only partly suppressed, i.e., 0.5 ppm at 25°C (E_{CI} ≈ 62%) and 25 ppm at 55°C (E_{CI} ≈ 55%).

3.1.2 | Intermittent Wetting

Electrochemical tests were conducted to examine the effect of intermittent wetting with hydrocarbon on corrosion inhibition. Figure 3 shows the CR of C1018 at 25°C and 55°C with intermittent oil wetting and pure water wetting with and without CI addition. The CR were kept almost constant during the blank (without inhibitor, circle symbol series) pure water wetting tests, with values of about 2 mm/y and 5 mm/y for 25°C and 55°C, respectively. The CR did not change significantly after the steel specimen was exposed intermittently to the oil phase in the absence of CI at both 25°C and 55°C (triangle symbol series).

With the addition of 0.5 ppm THP-C14 at 25°C (which was below MSSC) and after the first oil-wetting stage as described in the experimental section, the CR of carbon steel decreased slightly from 0.8 mm/y to 0.5 mm/y (Figure 3[a], square symbol series). After the second oil-wetting stage, the CR remained somewhat similar with a final value around 0.4 mm/y. When compared with the behavior of inhibited steel without oil exposure (Figure 3[a], rhomboid symbol series), the final CR after the intermittent oil wetting were only slightly reduced compared to those observed in the absence of oil.

Table 3. *Steady-State CR of C1018 Steel Inhibited with Various THP-C14 Concentrations in Pure Water Wetting Experiments (5 wt% NaCl Saturated with CO_2, pH 4.5) at 25°C and 55°C*[26(A)]

Temperature	CI Conc. (ppm_w)	CR (mm/y)	Inhibitor Efficiency (%)
25°C	0	2.01±0.13	–
	0.5	0.75±0.13	62±9
	1	0.29±0.07	85±4
	4	0.11±0.02	94±1
	8	0.09±0.02	95±1
	25	0.08±0.01	96±1
55°C	0	4.81±0.22	–
	8	2.28±0.17	52±6
	25	2.17±0.20	55±6
	50	0.57±0.11	88±3
	70	0.08±0.01	98.3±0.3

(A) Error bars indicate the max and min CR of repeated experiments.

On the other hand, at 55°C with the addition of 25 ppm THP-C14 (concentration also below MSSC), the CR decreased significantly after the first and second oil-wetting stages reaching a final value of about 0.07 mm/y (Figure 3[b], square symbol series). In this case, the contact with hydrocarbon promoted a very important synergistic effect on corrosion inhibition as seen from the comparison between the CR after intermittent oil wetting and those measured without oil (Figure 3[b], rhomboid series). The corrosion inhibition efficiency yielded about 98%, although the used inhibitor concentration was below the MSSC and the inhibitor efficiency in pure aqueous media was only around 55%.

3.2 | Potentiodynamic Sweeps

Figure 4 shows sets of potentiodynamic polarization curves for the steel C1018 exposed with the addition of THP-C14 with 0.5 ppm at 25°C and 25 ppm at 55°C, with and without contact with oil. All of the curves were collected at the end of the full electro chemical tests in pure water-wetting and intermittent oil-wetting conditions.

The anodic and cathodic curves were somewhat similar for the samples exposed with and without intermittent wetting with oil and the addition of CI at 25°C (Figure 4[a]). However, in the inhibition tests at 55°C (Figure 4[b]), the intermittent contact with hydrocarbon retarded both the anodic and cathodic reactions, with an associated shift in the limiting cathodic current of the hydrogen evolution reaction. This indicates that the inhibitor film formed with 25 ppm THP-C14 at 55°C incorporated hydrocarbon during intermittent wetting periods, reducing the steel exposed area and retarding the mass transfer of corrosive species to the metal surface which promoted better inhibition.

3.3 | Electrochemical Impedance Spectroscopy Analyses

Both used inhibitor concentrations were below MSSC, but tests at 25°C (0.5 ppm THP-C14) and 55°C (25 ppm THP-C14) presented very different outcomes upon exposure to the oil phase showing negligible effect and pronounced synergistic enhancement, respectively. To further understand this difference, EIS was utilized to monitor the electrochemical behavior of the exposed surfaces.

Figure 5 displays Nyquist and Bode plots of the impedance spectra collected at 25°C with no CI (blank) and with 0.5 ppm THP-C14 in pure water wetting and intermittent oil wetting conditions. For pure water wetting tests, the impedance spectra were similar over time and exhibited in all cases a single capacitive time constant related to the corrosion process. The Nyquist plots (Figure 5[a]) showed this time constant as a depressed semicircle (with the center under the real axis), which is typically attributed to the inhomogeneous response of solid surfaces during corrosion[27-28] (i.e., due to the roughness and/or inhomogeneities in the rate of occurring electrochemical

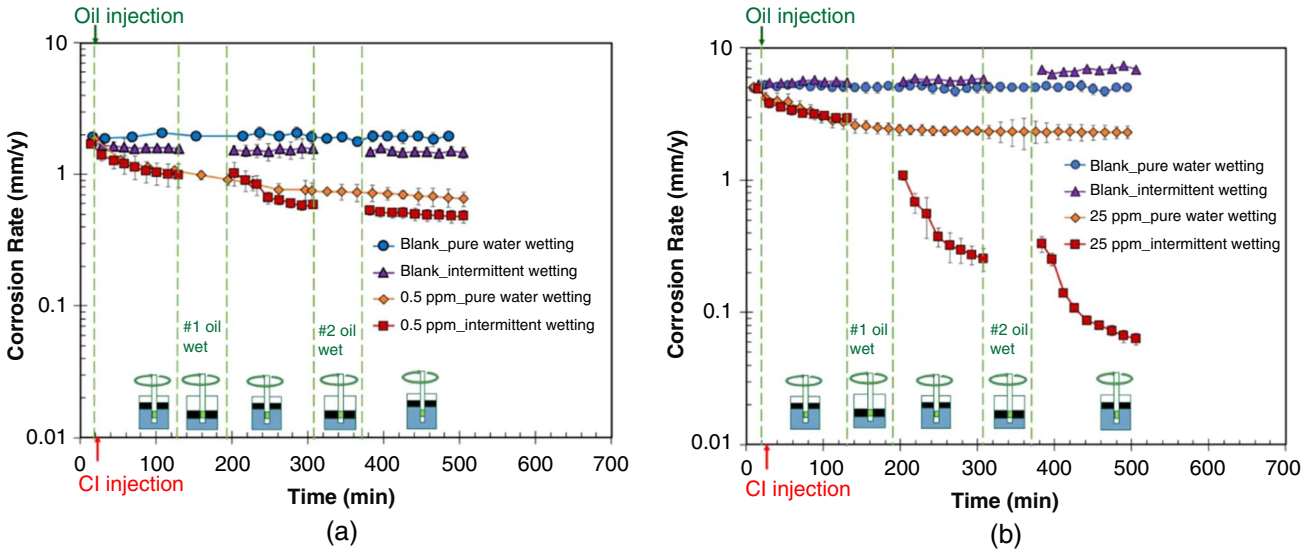

FIGURE 3. *The CR of C1018 steel with and without oil at (a) 25°C with no CI (blank) and 0.5 ppm THP-C14 and (b) 55°C with no CI (blank) and 25 ppm THP-C14. The sample was never in contact with oil during the pure water wetting experiment, i.e., oil was not added into the glass cell. The vertical dashed lines indicate different stages (oil-wet and water-wet) in intermittent wetting experiments.*

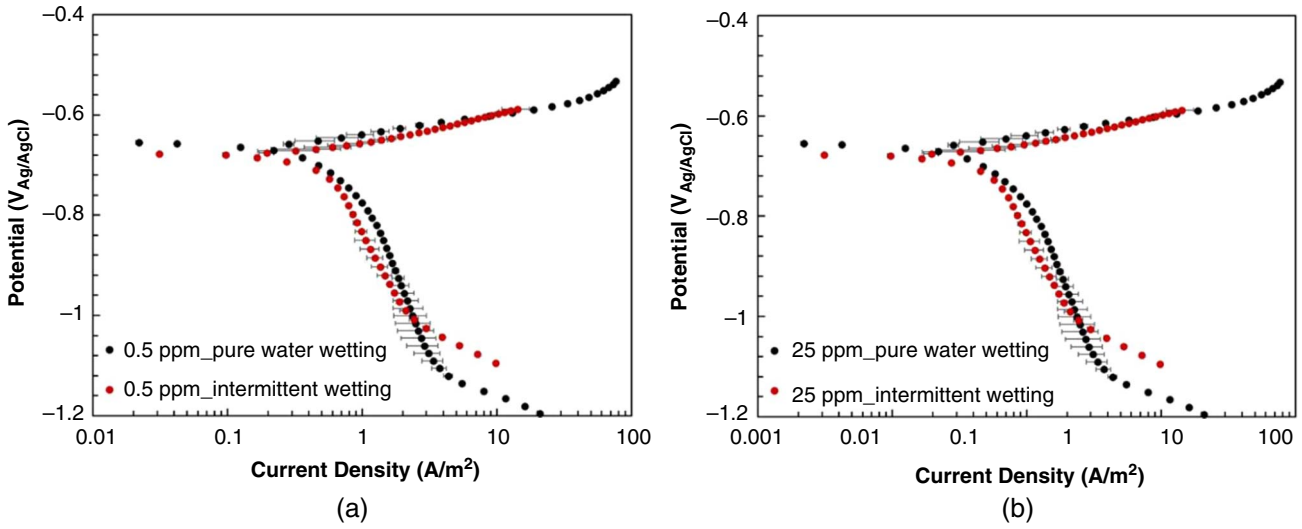

FIGURE 4. *Potentiodynamic polarization curves of C1018 steel with the addition of THP-C14 with (a) 0.5 ppm at 25°C and (b) 25 ppm at 55°C, with and without intermittent oil wetting.*

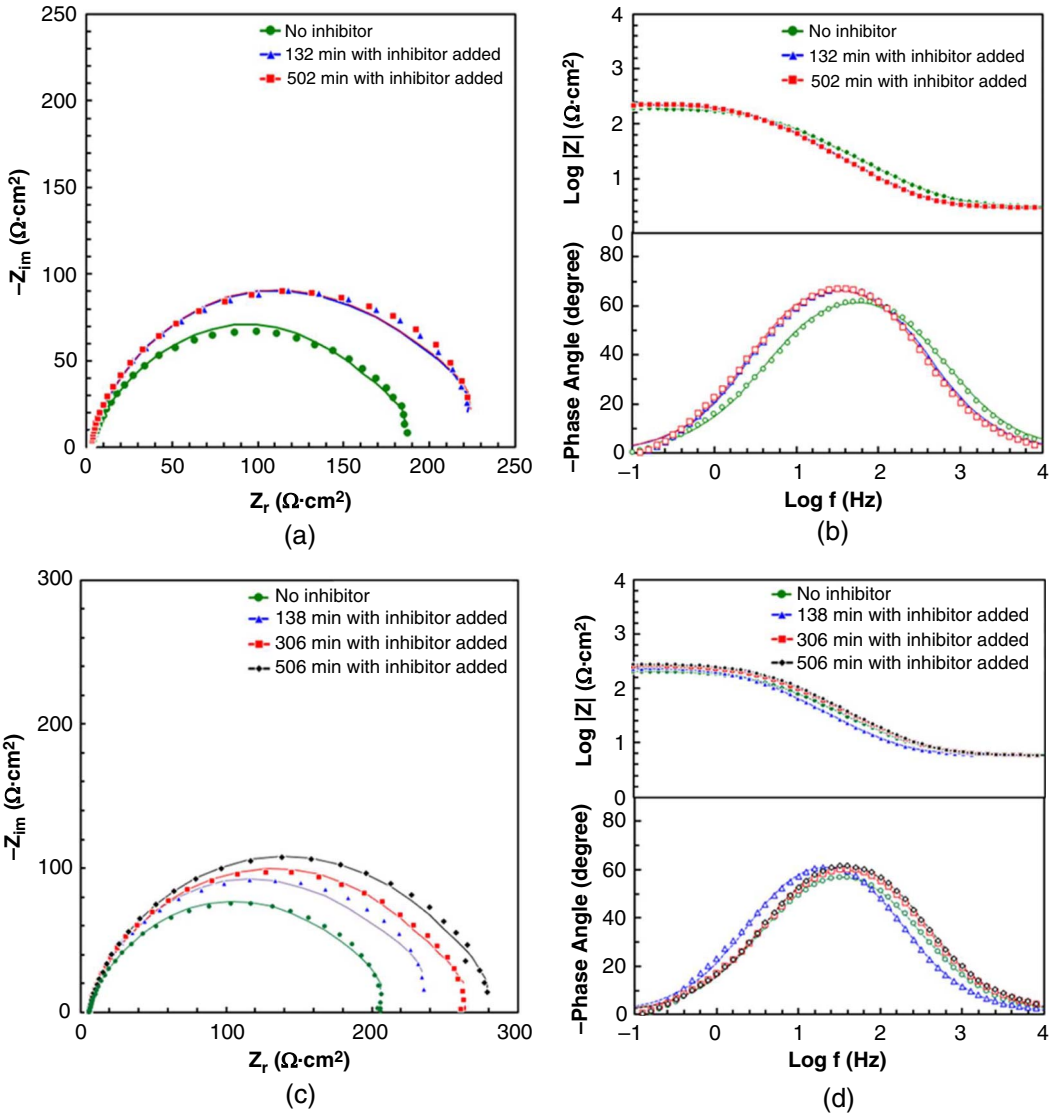

FIGURE 5. *Nyquist and Bode plots of EIS spectra of C1018 steel exposed at 25°C with 0.5 ppm THP-C14: (a) and (b) correspond to pure water wetting tests, (c) and (d) are from intermittent wetting tests. Symbols are experimental results and solid lines are fitting results.*

reactions). The impedance modulus at low frequencies increased with the addition of CI and then, it did not change significantly after 8 h of exposure (Figure 5[b]). Similarly, only one time constant was noted in the intermittent oil wetting experiments with CI as shown in Figures 5(c) and (d).

The impedance spectra for both pure water wetting and intermittent wetting tests were fitted using a Randles equivalent electrical circuit, as shown in Figure 6(a), where R_s is the electrolyte resistance, R_{ct} is the charge transfer resistance, and C_{dl} is the double-layer capacitance. It is noteworthy that when the inhibitor was added into the system, two factors contributed to the measured capacitance: the double layer (inhibitor-free) capacitance and a capacitance associated with the adsorbed inhibitor. The relative contribution of each capacitance component depends on the inhibitor coverage.[29] A constant phase element (CPE) was used in place of a perfect capacitor to model the dielectric behavior of the double layer to account for the typical nonideal deviation of solid metal electrodes[30]

$$Z_{CPE} = \frac{1}{Q(j\omega)^{\alpha}} \quad (3)$$

where Z_{CPE} is the impedance of CPE, ω is the angular frequency of the applied alternate voltage, j is the imaginary unit, and Q and α are the CPE magnitude and exponent describing the CPE, respectively. The calculation of the effective double layer capacitance (C_{dl}) linked to the CPE was performed utilizing the following equation[31]

$$C_{dl} = Q_{dl}^{1/\alpha_{dl}} \left(\frac{R_s R_{ct}}{R_s + R_{ct}} \right)^{(1-\alpha_{dl})/\alpha_{dl}} \quad (4)$$

The fitted values of the equivalent circuit parameters for the EIS data in Figure 5 are listed in Table 4. For the pure water wetting experiments, the R_{ct} increased after the first 2 h of exposure in the inhibited solution and then, it showed a slight growth during the remainder of the test. This pointed out that at the used concentration (0.5 ppm), the adsorption of inhibitor molecules only produced a moderate reduction of the active metal surface area. The behavior was similar for intermittent wetting conditions, where there was a moderate increase of R_{ct} with time due to inhibitor adsorption, and no significant changes in the impedance parameters were observed after the two oil-wetting stages.

Figure 7 shows Nyquist and Bode plots of the impedance spectra measured at 55°C with no CI (blank) and 25 ppm THP-C14 in pure water wetting and intermittent oil wetting conditions. For pure water wetting tests, one time constant was observed with and without inhibitor addition (Figures 7[a] and [b]). The low-frequency impedance increased in the first approximately 2 h after CI injection and remained stable for longer times. In intermittent wetting experiments (Figures 7[c] and [d]), the EIS spectra before and after approximately 2 h of CI addition only in contact with the water phase behaved similar to those shown in Figures 7(c) and (d), with a single time constant and an increase of the low-frequency impedance after inhibition. However, after the first and the second oil-wetting stages, an additional time constant became evident at high-frequency range as clearly shown in the Bode plot of Figure 7(d). This indicates that the formed inhibitor film interacted with the hydrocarbon, causing a modification in the electrode/electrolyte interfacial structure and increasing impedance significantly in the entire range of measured frequencies. In some cases, adsorbed inhibitor films can effectively incorporate hydrocarbon molecules forming a more effective barrier against the diffusion of corrosive species toward the metal surface.[13] These enhanced organic films can usually influence the high-frequency EIS response due to their dielectric behavior as seen in Figure 7(d), while the faradaic processes at the interface between the steel substrate and electrolyte are observed at mid/low frequencies.

The EIS spectra for the tests at 55°C were modeled using the equivalent circuit in Figure 6(a) for the pure water wetting behavior, and the circuit in Figure 6(b) for the postoil intermittent wetting response. The equivalent circuit in Figure 6(b) represents a porous organic (inhibitor + hydrocarbon) film on the carbon steel substrate, where R_{pore} is the resistance of the film pores and C_{film} is the capacitance of the

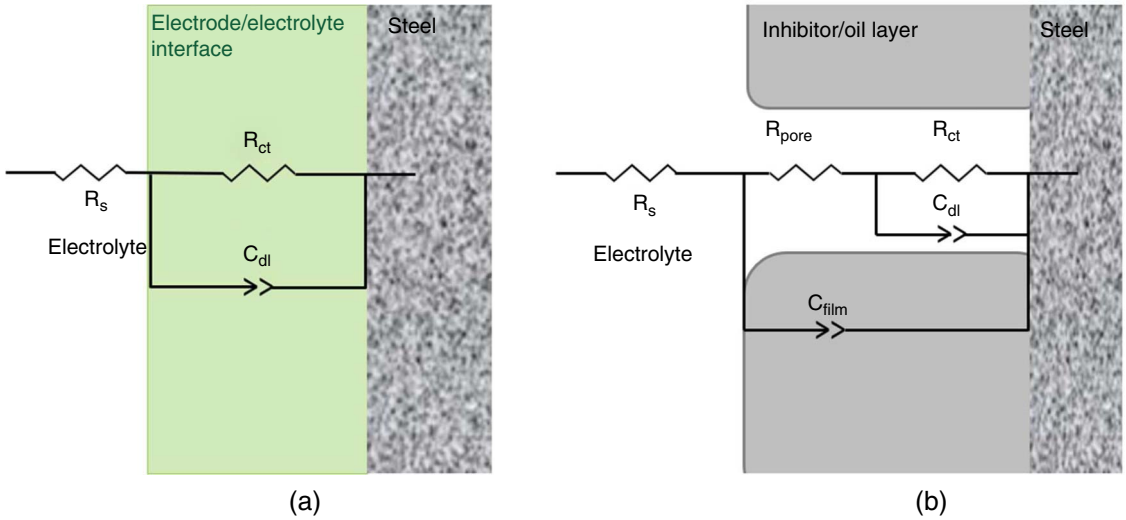

FIGURE 6. *Different equivalent circuits used for the modeling of the impedance data. (a) Equivalent circuit for experiments without oil (pure water wetting), where R_s represents electrolyte resistance, C_{dl} represents the capacitance of the double layer at the electrode/electrolyte interface, and R_{ct} represents the impedance of the faradaic reaction at the electrode/electrolyte interface. (b) Equivalent circuit for experiments after oil wetting, where R_{pore} represents the resistance of the surface film pores and C_{film} represents the capacitance of the surface film.*

Table 4. *Fitting Parameters of Equivalent Circuit Modeling of EIS Spectra for C1018 Steel Exposed at 25°C with 0.5 ppm THP-C14*[(A)]

Experiment	Time (min)	R_s (Ω)	R_{ct} (Ω·cm^2)	C_{dl} (μF/cm^2)	χ^2 ×10^{-4}
Pure water wetting	15	2.0	179	232	2.75
	132	1.8	223	216	0.24
	308	1.7	224	255	0.77
	502	1.9	237	279	1.12
Intermittent wetting	15	1.9	218	257	0.42
	138	2.0	225	286	0.78
	306	2.1	243	228	0.73
	506	2.1	272	211	0.46

[(A)] Time corresponds to Figure 3(a).

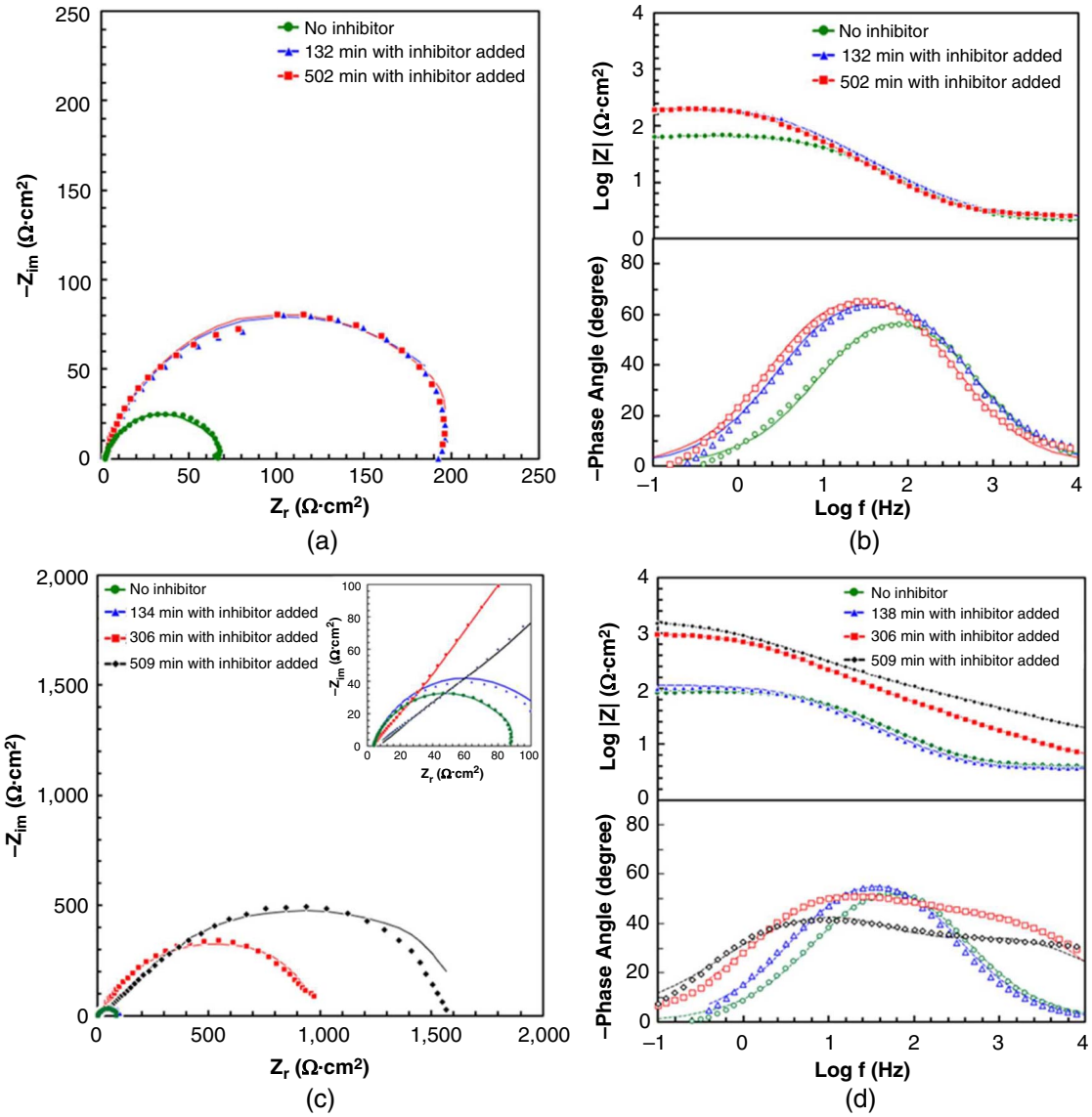

FIGURE 7. *Nyquist and Bode plots of EIS spectra of C1018 steel exposed at 55°C with 25 ppm THP-C14: (a) and (b) correspond to pure water wetting experiments, (c) and (d) are from intermittent wetting experiments. Symbols are experimental results and solid lines are fitting results.*

film.[32] The porous model was chosen based on its simplicity and on the fact that it is commonly used in inhibitor studies.[33-34] While other models may provide alternative explanations, the inhibitor + hydrocarbon film buildup process was analogized as the reverse of coating breakdown (as shown in Figure 6[b]). As mentioned above, CPEs were used instead of ideal capacitances to account for nonideal deviations. The effective double-layer capacitance, associated with the parameter C_{dl}, was determined using Equation (4), while the effective film capacitance was determined using the following expression[35]

$$C_{film} = Q_{film}^{\frac{1}{\alpha_{film}}} R_s^{\frac{1-\alpha_{film}}{\alpha_{film}}} \quad (5)$$

where Q_{film} and α_{film} are the pseudo capacitance and exponent (CPE parameters) of the film and R_s is the solution resistance. The fitted values of the impedance parameters are listed in Table 5. In the case of the pure water wetting condition, R_{ct} increased after the first 2 h of CI injection and remained similar over time. The increase of R_{ct} with the applied inhibitor concentration (25 ppm) indicated that inhibitor molecules adsorbed on the metal surface, blocking active area moderately and thereby decreasing the CR.

For intermittent wetting experiments, as shown in Table 5, R_{ct} increased and after the first hours of CI injection, similar to the initial stage of pure water wetting tests. However, after the first contact with oil and following exposure to the inhibited solution (ca. 306 min of the test), R_{ct} increased further around four times (from 223 Ω·cm^2 to 903 Ω·cm^2) and C_{dl} decreased about a similar factor (from 255 μF/cm^2 to 67.2 μF/cm^2), indicating a significant decrease of the exposed active metal surface. In addition, the time constant ($R_{pore} \times C_{film}$) emerged after the interaction with hydrocarbon due to the more insulating capabilities of the formed film. After the second oil-wet stage and later exposure to the inhibited solution (ca. 509 min of the test), R_{ct} and C_{dl} increased and decreased by almost a factor of 2, respectively, which indicated a further reduction of the active area. The capacitance of the film (C_{film}) also decreased. A simple parallel plate model can be used to assess the physical factors involved in the capacitance values of the formed organic film:[33,36]

$$C_{film} = \frac{\varepsilon_{film}\varepsilon_o A}{d_{film}} \quad (6)$$

where A is the total area of the electrode and ε_o is the permittivity of vacuum (~9×10^{-14} F/cm). As shown in Equation (6), the film capacitance is directly proportional to the dielectric constant of the inhibitor-hydrocarbon film (ε_{film}), and inversely proportional to the film thickness (d_{film}). The decreasing trend of C_{film} with time could be due to the changes in the dielectric properties of the film (ε_{film}), however, this cannot be directly measured. The decreasing trend of C_{film} with time and repeated contact with hydrocarbon could be mainly explained by an increase in the thickness of the protective film.[13] This is in line with the observed higher film pore resistance (R_{pore}) due to the larger diffusion path produced by the thicker film.

The precursor inhibitor film, which was likely formed only by a monolayer of inhibitor molecules adsorbed on the metal surface, moderately covered the active area and did not present a low capacitance because of its small thickness (i.e., few nanometers). Therefore, this behavior was captured in the EIS spectra as only one time constant related to the inhibited corrosion process. However, in this case, the further interaction with oil allowed the incorporation of hydrocarbon molecules that resulted in an enhanced thicker and less porous organic film which significantly improved corrosion inhibition. Interestingly, this phenomenon did not occur in the inhibition experiments with intermittent oil wetting at 25°C, where the same moderate inhibition behaviors with one-time constant spectra were recorded regardless of the exposure to hydrocarbon.

Although the inhibitor concentrations used at 25°C and 55°C were both intentionally selected to be below MSSC as an attempt to explore any synergistic effect of contact with hydrocarbon, the results were drastically different. Therefore, an extra experimental method was used to examine the affinity of inhibited steel surfaces with oil upon temperature and inhibitor concentration.

3.4 | Contact Angle Measurements

The characterization of the affinity of inhibited steel surfaces with the eventual contact with the hydrocarbon phase was very important to complement the electrochemical analyses above. The intermittent wetting CR results showed significant differences depending on the experimental temperature. Contact angle measurements were performed to determine the effect of CI on the hydrophilicity/hydrophobicity of the steel surface and to identify if this behavior was temperature dependent. Oil-in-water contact angles were measured at 25°C and 55°C on C1018 steel surfaces after injecting an LVT 200 oil droplet into the brine phase containing different concentrations of THP-C14 inhibitor from 0 ppm to 25 ppm. Figure 8 shows representative pictures of the measured sessile oil droplets on the different steel surfaces. The angle

Table 5. *Fitting Parameters of Equivalent Circuit Modeling of C1018 Steel Exposed at 55°C with 25 ppm THP-C14*[(A)]

Experiment	Time (min)	R_s (Ω)	R_{ct} (Ω·cm^2)	C_{dl} (μF/cm^2)	R_{pore} (Ω·cm^2)	C_{film} (μF/cm^2)	$\chi^2 \times 10^{-4}$
Pure water wetting	15	0.7	66.4	356	–	–	1.27
	132	0.8	198	272	–	–	0.35
	308	0.9	210	326	–	–	1.38
	502	0.9	202	376	–	–	2.08
Intermittent wetting	16	1	87.9	326	–	–	0.43
	134	1.1	223	255	–	–	0.71
	306	1.12	903	67.2	75.6	6.3	0.78
	509	1.7	1,639	37.4	104	0.5	3.66

[(A)] Time corresponds to Figure 3(b).

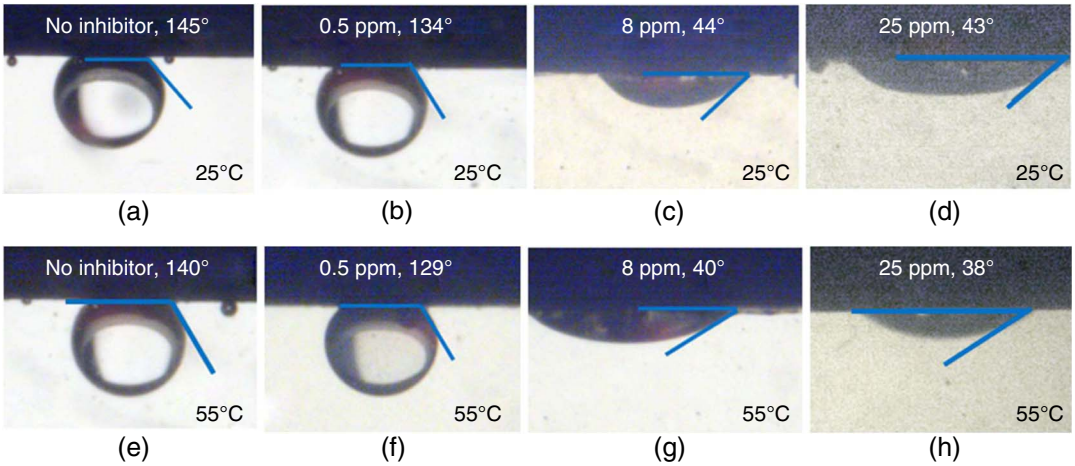

FIGURE 8. *Pictures of oil-in-water contact angle in the brine phase with different concentrations of THP-C14 (from 0 ppm to 25 ppm) at (a) through (d) 25°C and (e) through (h) 55°C. Used inhibitor concentrations and measured contact angles are labeled on each picture.*

between the tangent line of the droplet contact edge and the steel surface plane is the oil-in-water contact angle as a marked reference in Figure 8. The average measured contact angle value was also noted for each condition in the same figure. For both temperatures, the contact angle of the oil droplets decreased upon the addition of inhibitor from 140° to 145° (Figures 8[a] and [e]), which denoted hydrophilic surfaces, to 38° to 43° (Figures 8[d] and [h]), which denoted hydrophobic surfaces. This drastic change of wettability was produced somewhere in the inhibitor concentration range from 0.5 ppm to 8 ppm.

When there is no inhibitor added to the brine, it is very difficult for the inert hydrocarbon chains in the oil phase to displace water molecules and spread out on the steel surface, because carbon steel is hydrophilic (as illustrated in Figures 8[a] and [e]). However, CIs can change the wettability of the steel surface, transforming it from hydrophilic to hydrophobic. This transformation occurs as a hydrophobic adsorbed layer forms on the steel surface. The hydrophilic heads of the inhibitor molecules adsorb on the steel surface, and their hydrophobic tails orientate toward the solution. Those hydrophobic tails repel water and can attract hydrocarbon molecules through Van der Waals interactions, leading to oil wetting. This behavior was captured with the addition of 8 ppm or larger concentrations of THP-C14, where the sessile oil droplets spread widely on the steel surface. Moreover, there was no significant effect of temperature on the measured oil-in-water contact angles, which meant that the alteration of steel surface wettability was not temperature-dependent.

3.5 | General Remarks

The wettability tests above shed light on the cause of the very different behaviors recorded during the inhibition experiments with intermittent oil wetting at different temperatures using CI concentrations below MSSC that provided similar low inhibition efficiencies in pure water wetting conditions. Although at 55°C the use of 25 ppm inhibitor was not satisfactory, it was enough to turn the inhibited surface hydrophobic (Figure 8[d]) so the oil phase potentially incorporated in the adsorbed inhibitor layer during contact, and was carried along when the specimen was returned to brine phase. The hydrocarbon incorporation due to modified surface wettability could promote further additive inhibition, reducing greatly the CR observed in Figures 3(b), 4(b), and 7. For a better understanding of this scenario, Figure 9 shows some simplified schemes describing the potential mechanisms involved in the inhibition of intermittent oil contact. During the first water-wetting stage (i.e., Figure 9[c]), the substrate surface becomes hydrophobic after 25 ppm THP-C14 injection, possibly due to the formation of a film with a relatively small distance between adsorbed inhibitor molecules with their aliphatic tails mostly oriented opposite to the metal surface. Subsequently, when the sample is exposed to the oil phase during the first oil-wetting stage (Figure 9[d]), the inhibitor readily interacts with the hydrocarbon which incorporates the aliphatic chains of the adsorbed molecules and forms an oil-containing inhibitor surface film that then keeps improving within the first hour of re-exposure to the inhibited solution (i.e., Figure 3[b], square symbol series). Thus, after the sample is repeatedly wetted by water and oil during the second water-wetting and oil-wetting stages and the last third water-wetting stage, more entangled oil further promotes corrosion inhibition.

However, such an additive effect was not observed at 25°C with 0.5 ppm THP-C14. In this scenario, the substrate surface remains hydrophilic (oil-in-water contact angle higher than 90°, Figure 8[b]) after inhibitor injection during the first water-wetting stage, possibly due to a relatively low density of adsorbed molecules in the formed inhibitor film (Figure 9[a]). Then, when the sample is exposed to the oil phase during the first oil-wetting stage (Figure 9[b]), the adsorbed inhibitor promotes limited interaction with the hydrocarbon due to insufficient aliphatic sites on the surface, and hydrocarbon does not incorporate or adhere to the inhibitor film. Thus, the oil does not entangle in the adsorbed inhibitor film even after repeated intermittent wetting cycles and cannot promote significant additional corrosion inhibition (Figure 3[a]).

The above results and discussion demonstrate that the MSSC, which is usually used as practical inhibitor dosing guidance in pure water wetting without oil, can be a very conservative parameter to characterize effective corrosion inhibition of carbon steel in intermittent oil-water wetting in certain circumstances. Based on the experimental results at 55°C, even though the used inhibitor concentration of 25 ppm was below the MSSC (i.e., between 50 ppm and 70 ppm), the corrosion inhibition performance with THP-C14 was greatly enhanced in

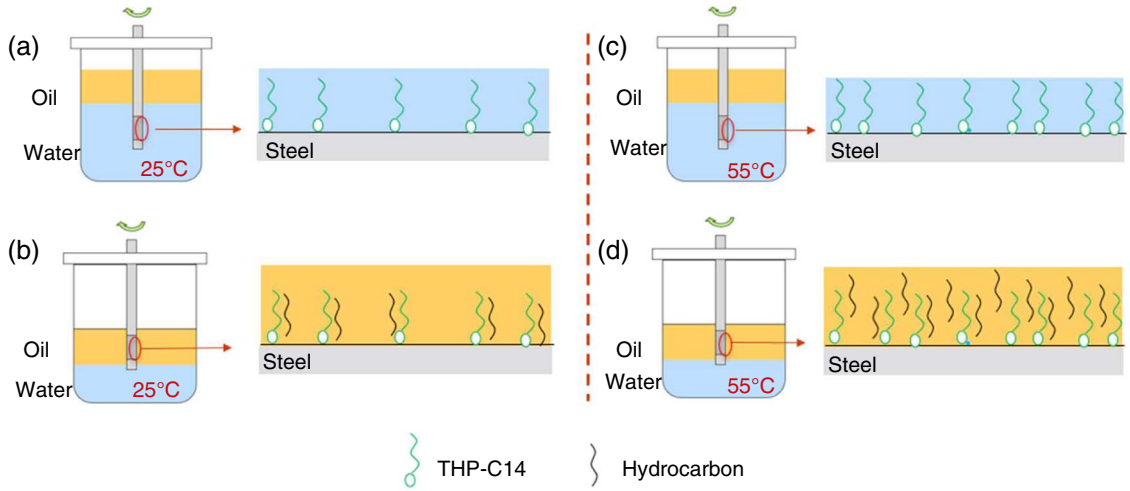

FIGURE 9. *The proposed mechanisms at 25°C and 0.5 ppm THP-C14 (a) water-wetting stage and (b) oil-wetting stage, and at 55°C and 25 ppm THP-C14, (c) water-wetting stage, and (d) oil-wetting stage.*

systems. where the steel surface was intermittently wetted with the oil phase.

The MSSC represents the minimum critical bulk concentration of CI required for saturating the metal surface with adsorbed inhibitor molecules.[37] This saturation leads to a minimal CR and maximum inhibition efficiency. Determining MSSC involves comparing the stable CR of metal specimens exposed to various CI concentrations, it does not correlate with the sample surface wettability as shown here and discussed elsewhere.[18] In the past few years, there has been more awareness of the issue of characterizing surface wettability as an important assessment for CI products for hydrocarbon-water environments.[38-39] However, there is no well-established procedure or way yet to classify or quantify the wettability benefit on CI performance in the presence of hydrocarbons. In this regard, the corrosion test setup (glass cell with alternating liquid contact and use of various electrochemical techniques) plus complementary wettability studies via sessile contact angles have offered a good framework to obtain relevant information. Thus, future work will aim efforts to characterize this phenomenon over a broader range of conditions (i.e., temperatures and CI concentrations) and different CIs pointing out the issue that a sort of new parameter like a "minimum wettability change" concentration (MWCC) can be a better indicator than MSSC for optimum inhibition performance in some applications with intermittent oil-water wetting. For a given CI, there might be conditions, where MWCC is significantly lower than MSSC rendering the latter overconservative and antieconomic to achieve similar optimum corrosion inhibition.

CONCLUSIONS

The impact of intermittent wetting on corrosion inhibition of carbon steel in oil-water systems was investigated at temperatures of 25°C and 55°C, utilizing various concentrations of CI. Some main points from this research are summarized as follows:

➢ The performance of THP-C14 CI was significantly enhanced when the steel surface was periodically wetted with oil only in the tests at 55°C, although the used inhibitor concentrations were below the MSSC in tests run at both 25°C and 55°C.

➢ At 55°C and 25 ppm THP-C14, the intermittent contact with hydrocarbon retarded both the anodic and cathodic reactions compared with the pure water wetting inhibition conditions, with an associated shift in the limiting cathodic current. This indicated that the oil enhanced the precursor adsorbed inhibitor film reducing the steel exposed area and retarding the mass transfer of corrosive species to the metal surface, promoting better inhibition.

➢ The inhibitor film formed at 55°C incorporated hydrocarbon and produced an improved protective film that changed the electrode/electrolyte interfacial structure which was observed as an extra high-frequency time constant in the measured EIS spectra. EIS data suggested the formation of a thicker and less porous film when oil is present. This beneficial effect was not observed in the tests at 25°C and 0.5 ppm THP-C14. The used inhibitor produced a significant change in the steel surface wettability for concentrations between 0.5 ppm and 8 ppm in pure water wetting conditions due to the formation of a hydrophobic inhibitor film. This phenomenon did not depend on temperature and did not relate to corrosion inhibition performance which is best for inhibitor concentrations equal to or greater than MSSC in the pure aqueous environment.

➢ The enhanced inhibition with direct exposure to hydrocarbon (intermittent wetting) could be related to the wettability change of the steel surface to hydrophobic allowing the attachment of the oil phase and the formation of improved protective films. Final CR and overall inhibitor performance in this scenario were as good as those achieved for inhibitor concentrations similar to or larger than MSSC in pure water wetting conditions.

➢ Metal surface saturation concentration would not be an appropriate indicator to assess the performance or the optimum needed dosage of a given CI environment with oil-water intermittent wetting in some cases, because it can be very conservative. Instead, a parameter like a "minimum wettability change" inhibitor concentration can be a better gauge to define the optimum dosage in this scenario.

ACKNOWLEDGMENTS

This project has been supported by TotalEnergies transversal R&D project (MANA Project). The authors would like to thank Alexis Barxias and Cody Shafer for their technical support.

References

1. M.B. Kermani, D. Harrop, *SPE Prod. Facil.* 11 (1996): p. 186-190.
2. J. Cai, C. Li, X. Tang, F. Ayello, S. Richter, S. Nešić, *Chem. Eng. Sci.* 73 (2012): p. 334-344.
3. Y. Xiong, B. Brown, B. Kinsella, S. Nešić, A. Pailleret, *Corrosion* 70 (2014): p. 247-260.
4. V. Otieno-Alego, N. Huynh, T. Notoya, S.E. Bottle, D.P. Schweinsberg, *Corros. Sci.* 41 (1999): p. 685-697.
5. D. Chebabe, Z. Ait Chikh, N. Hajjaji, A. Srhiri, F. Zucchi, *Corros. Sci.* 45 (2003): p. 309-320.
6. F. Bentiss, M. Lagrenee, M. Traisnel, J.C. Hornez, *Corros. Sci.* 41 (1999): p. 789-803.
7. C. Li, S. Richter, S. Nešić, *Corrosion* 70 (2014): p. 958-966.
8. S. Yang, S. Richter, W. Robbins, S. Nešić, *Corrosion* 3 (2012): p. 2554-2568.
9. W.L. Ma, H.X. Wang, R. Barker, N. Kapur, Y. Hua, A. Neville, *Corros. Sci.* 187 (2021): p.1-12.
10. M. Meeusen, L. Zardet, A.M. Homborg, M. Lekka, F. Andreatta, L. Fedrizzi, B. Boelen, H. Terryn, J.M.C. Mol, *J. Electrochem. Soc.* 166 (2019): p. C3220-C3232.
11. E.P.M. van Westing, G.M. Ferrari, J.H.W. de Wit, *Corros. Sci.* 36 (1994): p. 1323-1346.
12. Z. Belarbi, J.M. Dominguez Olivo, F. Farelas, M. Singer, D. Young, S. Nešić, *Corrosion* 75 (2019): p. 1246-1254.
13. J. Sonke, W.M. Bos, "Oil and Gas Field Corrosion Inhibitor Performance Validation Implementation of EIS," CORROSION 2018, paper no. 10636 (Houston, TX: NACE, 2018).
14. Y. He, X. Wang, D. Young, M. Mohamed-Said, S. Ren, M. Singer, *J. Electrochem. Soc.* 170 (2023): p. 111502.
15. R.G. dos Santos, R.S. Mohamed, A.C. Bannwart, W. Loh, *J. Pet. Sci. Eng.* 51 (2006): p. 9-16.
16. ASTM G205-16, Standard Guide for Determining Corrosivity of Crude Oils (American Society for Testing and Materials), ASTM Book of Standards (n.d.), p. 1-10.
17. NACE International, "Corrosivity of Crude Oil under Pipeline Operating Conditions" (Houston, TX: NACE, 2012), ISBN: 157-590-2575.
18. G. Schmitt, N. Stradmann, "Wettability of Steel Surfaces at CO_2 Corrosion Conditions I Effect of Surface Active Compounds in Aqueous and Hydrocarbon Media," CORROSION 98, paper no. 98028 (Houston, TX: NACE, 1998).
19. M. Foss, E. Gulbrandsen, J. Sjoˆblom, *Corrosion* 64 (2008): p. 905-919.
20. S. Papavinasam, A. Doiron, T. Panneerselvam, R.W. Review, *Corrosion* 63 (2007): p. 704-712.
21. Y. He, S. Ren, X. Wang, D. Young, M. Singer, Z. Belarbi, M. Mohamed-Saïd, S. Camperos, R. Khan Md, K. Cimatu, *Corrosion* 78 (2022): p. 625-633.
22. Z. Belarbi, F. Farelas, M. Singer, S. Nešić, *Corrosion* 72 (2016): p. 1300-1310.
23. A. Kahyarian, M. Singer, S. Nešić, *J. Nat. Gas Sci. Eng.* 29 (2016): p. 530-549.
24. T. Gardner, L.D. Paolinelli, S. Nešić, *Exp. Therm. Fluid Sci.* 102 (2019): p. 506-516.
25. S. Srinivasan, G.H. McKinley, R.E. Cohen, *Langmuir* 27 (2011): p. 13582-13589.
26. Y. He, S. Ren, X. Wang, D. Young, M. Mohamed-Said, B. Augusto Farah Santos, M. Eduarda Dias Serenario, M. Singer, *Corrosion* 80 (2024): p. 177-186.
27. M.P. Desimone, G. Grundmeier, G. Gordillo, S.N. Simison, *Electrochim. Acta* 56 (2011): p. 2990-2998.
28. D. Gopi, K.M. Govindaraju, L. Kavitha, *J. Appl. Electrochem.* 40 (2010): p. 1349-1356.
29. E. McCafferty, *Introduction to Corrosion Science* (New York, NY: Springer, 2010), p. 33-46.
30. M. Arunkumar, A. Paul, *ACS Omega* 2 (2017): p. 8039-8050.
31. G.J. Brug, A.L.G. van den Eeden, M. Sluyters-Rehbach, J.H. Sluyters, *J. Electroanal. Chem.* 176 (1984): p. 275-295.
32. M.E. Orazem, B. Tribollet, *Electrochemical Impedance Spectroscopy* (Hoboken, NJ: John Wiley & Sons, Inc., 2008), p. 61-72.
33. K. Marušić, H.O. Ćurković, H. Takenouti, *Electrochim. Acta* 56 (2011): p. 7491-7502.
34. S.L. Wu, Z.D. Cui, G.X. Zhao, M.L. Yan, S.L. Zhu, X.J. Yang, *Appl. Surf. Sci.* 228 (2004): p. 17-25.
35. B. Hirschorn, M.E. Orazem, B. Tribollet, V. Vivier, I. Frateur, M. Musiani, *Electrochim. Acta* 55 (2010): p. 6218-6227.
36. F. Mansfeld, C.H. Tsail, *Corrosion* 47 (1991): p. 958-963.
37. T. Murakawa, S. Nagaura, N. Hackerman, *Corros. Sci.* 7 (1967): p. 79-89.
38. Z.M. Wang, J. Zhang, *Corros. Rev.* 34 (2016): p. 17-40.
39. L.D. Paolinelli, A. Rashedi, J. Yao, M. Singer, *Chem. Eng. Sci.* 183 (2018): p. 200-214.